ISSN: 1992-8645 www.jatit.org E-ISSN: 1817-3195

A NEW APPROACH TO REPRESENT ROTATED HAAR-LIKE FEATURES FOR OBJECTS DETECTION

[1]MOHAMED OUALLA, [2]ABDELALIM SADIQ, [3]SAMIR MBARKI
Ibn Tofail University, Department of Informatics, Faculty of Sciences, Kenitra, Morocco
E-mail: [1]mohamed.oualla@taalim.ma, [2]sadiq.alim@gmail.com, [3]mbarki@hotmail.com

ABSTRACT

In this paper, we propose a new approach to detect rotated object at distinct angles using the Viola-Jones detector. Our method is based on two main steps: in the first step, we determine the rotated Haar-like feature by any angle (45°, 26.5°, 63.5° and others), this allowed us to obtain a very large number of Haar-like features for use them during the boosting stage. The normal Integral Image is very easy to be calculated, but for rotated Haar-like feature, their computation is practically very hard. For this reason, in second step, we propose a function to calculate an approximate value of rotated Integral Image at a generic angle. To concretize our method, we test our algorithm on two databases (Umist and CMU-PIE), containing a set of faces attributed to many variations in scale, location, orientation (in-plane rotation), pose (out-of-plane rotation), facial expression, lighting conditions, occlusions, etc.

Keywords: *Haar-Like Feature, Integral Image, Object Detection, Face Detection, Viola & Jones Algorithm.*

1. INTRODUCTION

Object detection has been one of the most studied topics in the computer vision literature. To detect an object in an image, the detector must have knowledge of the object characteristics. In fact, the most important step in the objects detection is the extraction of object features. Various approaches have been utilized in this literature such as Haar-Like features [4][5], color information, skin color [3], etc. In this paper we will focus on Haar-Like features.

There are many motivations for using features rather than the pixels directly. The most common reason is that features can act to encode ad-hoc domain knowledge that is difficult to learn using a finite quantity of training data. For this system there is also a second critical motivation for features: the feature based system operates much faster than a pixel-based system. [4]

The use of Haar-Like features has three challenges to be met. The first challenge is the extent of its efficiency in the detection of objects. Due to the non-invariant nature of the normal Haar-like features, classifiers trained with this method are often incapable of finding rotated objects. It is possible to use rotated positive examples during training, but such a monolithic approach often results in inaccurate classifiers [7]. For this reason Various methods have attempted to solve this problem by introducing inclined features, by 45° [8], 67,7° [9] [10] [11] [12], generic angles [45], in the learning boosting stage.

The second challenge of the use of Haar-Like features remains in how to present them practically. For normal features, their presentation is easy to achieve practically. Contrariwise, the presentation of rotated features is a big challenge because the presentation of an inclined rectangle, in an image, at an angle different to 0°, would cause a distortion of his sides, which makes the determination of integral image very hard.

The third challenge is manifested in how to calculate the integral image of a rotated feature by any angle. The normal Integral Image is very easy to be calculated, that is done by summing the pixels values above and to the left of the given pixel. But for rotated Haar-like feature, their computation is practically very hard; this is due to the distortion of their sides caused by their rotation. So the determination of the pixels forming these sides will be very difficult, and this will lose the Integral Image its simplicity and its quickness for which is defined by Viola & Jones.

In this paper we present two algorithms. The first determine the rotated haar-like features by any angles. The second allows us to approximate the

Journal of Theoretical and Applied Information Technology
10th August 2015. Vol.78. No.1

ISSN: 1992-8645 www.jatit.org E-ISSN: 1817-3195

rotated integral image at any angle. We show that these algorithms are effective by giving some practical examples, tests and results of comparison with other methods.

The paper is organized as follows: a brief description of the Viola-Jones methods and algorithms are presented, including some important extensions added by other authors. Next the proposed method for determination of rotated Haar-like feature at a set of suitable angles is explained. The following section presents practical examples. Finally the conclusions point out the limitations and some challenges on a generic rotation invariant detector using Haar-like features.

2. RELATED WORK

Since their apparition by Papageorgiou et al. [1] that they have introduced a general framework for object detection using a Haar wavelet representation [2] until they become more famous when Viola and Jones [4][5][6] have proposed to use them for their face detection algorithm, Haar-like features has become an increasingly indispensable tool for extracting information that characterizes an elected object to be detected.

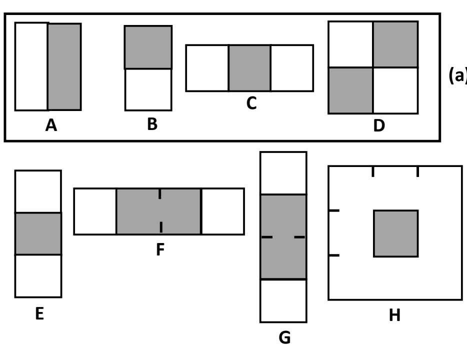

Figure 1: Example rectangle features shown relative to the enclosing detection window.

Figure 1-(a) shows the normal Haar-like features defined by Viola and Jones [4]. The principle of their algorithm, which is a boosting algorithm, is to classify an area of the image as face or non-face from multiple weak classifiers (a weak classifier is just a Haar-like feature with a weight) having a good classification rate slightly better than random classifier. These weak classifiers consist of summing pixels at select areas (rectangular) of the image and to subtract them with other. In order to reduce the computational cost of the summations, Viola & Jones introduced the integral image: Each point of the integral image can be computed once for an image. The integral image, denoted ii(x, y), at location (x, y) contains the sum of the pixel values above and to the left of (x, y) (see figure 2-a), formally with equation (1). Using the integral image, any rectangular sum can be computed in four array references (see figure 2-b). For example, to compute the sum of region A, the following four references are required: 4+1-(2+3).

$$ii(x,y) = \sum_{\substack{x' \leq x \\ y' \leq y}} i(x',y') \qquad (1)$$

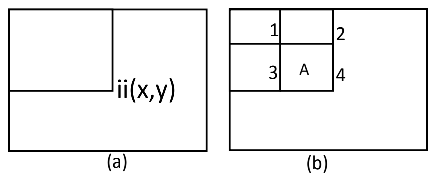

Figure 2: The integral image of (a) a point and (b) a rectangle

Viola and Jones used a customized version of Adaboost to aggregate the weak classifiers. One of the changes made to the algorithm was the creation of many layers (called cascades), each one being trained by several rounds of Adaboost to create strong classifiers that can detect if an area of an image contains the desired object or not.

Detectors trained by the group of features in figure 1, have shown their limitation to detect rotated objects. Therefore Lienhart et al. [8] introduced an extended set of twisted Haar-like feature at 45°. But also with this extension we cannot detect rotated objects by angles other than 45°. For this reason Barczack [9] proposes a new approach to detect rotated objects at distinct angles using the Viola-Jones detector. The use of additional Integral Images makes an approximation to the value of Haar-like features for any given angle. The proposed approach uses different types of Haar-like features, including features that compute areas at 45°, 26.5° and 63.5° of rotation. Barczak continued his work with Mossom [10][11] where they used angles which their tangents are rational numbers which allows the use of different angles. If we consider α one of these angles we will have α= arctan (Y/X) where X and Y are integers and X or Y is 1. With this method, the rotated objects by an angle arctan (Y/X) such that X and Y are different from 1, cannot be detected. Subsequently Ramirez et al [13] introduce the use of asymmetric Haar features, eliminating the

Journal of Theoretical and Applied Information Technology
10th August 2015. Vol.78. No.1

ISSN: 1992-8645 www.jatit.org E-ISSN: 1817-3195

requirement of equalized positive and negative regions in a feature. They propose Haar features with asymmetric regions that can have regions with either different width or height, but not both.

3. ROTATED HAAR-LIKE FEATURES

A detector trained by the features proposed by Lienhart et al [8] and those proposed by Barczak [9] can only be built by the angles 45°, 26.57°, 63.43° and others cited in [10][11]. And as mentioned above, this detector will have difficulties to detect rotated object by any other angle. The normal features and the rotated features are not mathematically equivalent in digital processing due to the fact that the rotated Integral Image needs slightly distorted rectangles to correctly compute an area.

Our idea is simple, and consists of scanning the window used during the training stage (base resolution of 24x24), and at the level of each point, determine all possible rectangles that are rotated by different angles. This current point represents the bottom-left corner of each rectangle found. Our method don't fix the number of angles to use from the beginning of training stage as they did the authors of [8], [9], [10] and [11]. The number of angles used varies from one window to another depending on its base resolution.

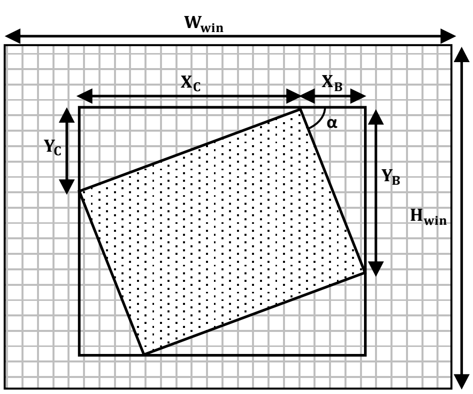

Figure 3: Representation of the rotated rectangle and its rectangle that encapsulates it

A general rotation, by any angle, cannot be easily implemented; therefore we define a restricted set of rotations that can be easily and effectively implemented. This set contains valid angles which represent the rotated rectangles preserving their integrity. A rotated Haar-like feature is a feature that has been rotated by a valid angle $\alpha = \arctan\left(\frac{Y_B}{X_B}\right) = \arctan\left(\frac{X_C}{Y_C}\right)$ where X_B, Y_B, X_C and Y_C are integers (figure 3). Such angles was used by Messom et al. [9] but with the restriction that X_B or Y_B and X_C or Y_C is 1, contrariwise, in our method these variables are positive integers that can have any value. The angles chosen are those having a rational tangent. A 45° rotated Haar-like feature is a special case of a feature which $X_B = Y_B$ and $X_C = Y_C$. Each rectangle is encapsulated by another normal (see figure 3) having the following size: $W=X_B+X_C$ and $H=Y_B+Y_C$ such as $\frac{Y_B}{X_B} = \frac{X_C}{Y_C}$, $H<H_{win}$ and $W<W_{win}$ knowing that W_{win} and H_{win} are, respectively, width and height of the training window (in our case we are using a base resolution of 24x24).

Indeed, in a window training $Win(W_{win},H_{win})$, a rotated rectangle (ABCD) is a rectangle witch its bottom-left corner is $A(x_A,y_A)$ and which its sides [AB] and [AC] form two areas, respectively, B_{area} and C_{area} (figure 4). Each area consists of a set of points, each point represents a pixel. The two sets may be expressed in the following way.

$$B_{area} = \{P_B(x_{P_B}, y_{P_B}) \in Win / x_A < x_{P_B} < W_{win} \text{ and } y_A < y_{P_B} < H_{win}\} \quad (2)$$

$$C_{area} = \{P_C(x_{P_C}, y_{P_C}) \in Win \,/\, 0 \le x_{P_C} < x_A \text{ and } y_A < y_{P_C} < H_{win}\} \quad (3)$$

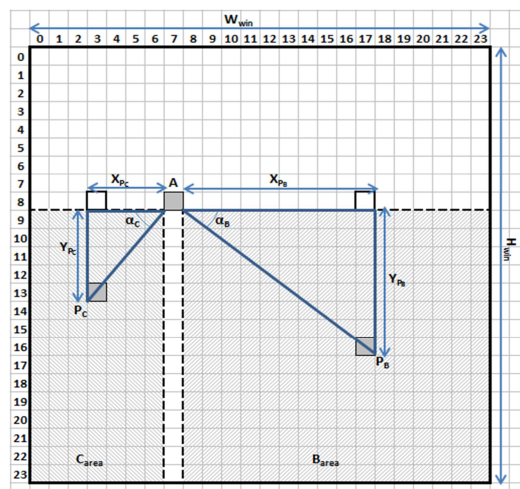

Figure 4 : Determination of the valid rectangles for a point $A(x_A,y_A)$

Therefore, to determine the valid rectangles at level of point $A(x_A,y_A)$ (i.e. the rectangles that their integrity is preserved, otherwise, those for which their angles are rights), we must determine the couples (P_B ,α_B) such as α_B is possible angle of the orientation of the side

ISSN: 1992-8645 www.jatit.org E-ISSN: 1817-3195

$[AP_B]$ (figure 4). As already mentioned above, $\alpha_B = \arctan\left(\frac{Y_B}{X_B}\right)$ Where:

$$Y_B = |Y_{P_B} - Y_A| \text{ and } X_B = |X_{P_B} - X_A|$$

In the same way, we determine the couples (P_C, α_C). The couples of the two areas can be expressed as follows:

$$B_\alpha = \{(P_B, \alpha_B) \;/\; P_B \in B_{area} \text{ and } \alpha_B = \arctan\left(\frac{Y_B}{X_B}\right) \text{ where } Y_B = |y_{P_B} - y_A| \text{ and } X_B = |x_{P_B} - x_A|\} \quad (4)$$

$$C_\alpha = \{(P_C, \alpha_C) \;/\; P_C \in C_{area} \text{ and } \alpha_C = \arctan\left(\frac{Y_C}{X_C}\right) \text{ where } Y_C = |y_{P_C} - y_A| \text{ and } X_C = |x_{P_C} - x_A|\} \quad (5)$$

Therefore, the rotated valid rectangles, called Rhl_A, by an angle α_v are those in which their side $[AP_B]$ is rotated by that same angle in such a way that there is a side $[AP_C]$ rotated by an angle α_C provided that these two angles are complementary, Otherwise:

$$Rhl_A = \{(P_B, P_C, \alpha_v) \;/\; (P_B, \alpha_v) \in B_\alpha \text{ and } \exists\, (P_C, \alpha_C) \in C_\alpha \text{ such as } \alpha_v + \alpha_C = 90°\} \quad (6)$$

As a final result, all rotated rectangles that we can obtain from a training window Win is:

$$Rhl = \cup_{A \in Win} Rhl_A. \quad (7)$$

Given that the base resolution of the detector is 24x24, the exhaustive set of rotated rectangle features is quite large, 130000.

4. INTEGRAL IMAGE

4.1 Problematic

The normal Integral Image for a given normal feature is very easy to be calculated. This is done by summing the pixels values above and to the left of the given pixel (figure 2). For rotated integral image, their computation is, practically, very hard.

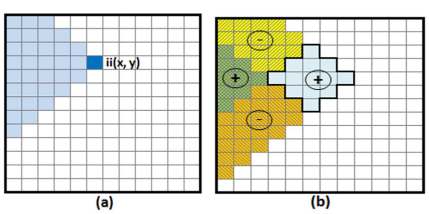

Figure 5: Twisted Integral image representation. (a) The value of the twisted Integral Image at point (x,y). (b) Calculation scheme of the pixel sum of rotated rectangles by 45°.

Lienhart et al. [8] have given a method to calculate the rotated Integral Image by 45° (as they named it: *Twisted Integral Image*) as shown in figure 5. The computing operation for all the features follows the same rule; the value of a pixel is calculated by summing the pixels values obtained by moving, since this pixel, firstly from one step to the left and then another on top and secondly from one step to the left and then another down (figure 5(a)). However, for the rotated feature by an angle different of 45°, the possibility of finding a rule to browse the pixels of a rectangle becomes very difficult.

For this raison, and because we have to deal with thousands of rectangles, obtained by our algorithm, representing different angles and dimensions, we propose a function to calculate an approximate value of rotated integral image at a generic angle.

4.2 Rotated Feature Computation

4.2.1 Principle

The principle of our technique consists in dividing each normal rectangle, which encapsulates the rotated rectangle, in several other normal. Thereafter, according to the integral image of these rectangles, we calculate that of the rotated rectangle.

A Haar-Like feature is a rectangle composed either of 2, 3 or 4 rectangles (see figure 1). Each rectangle, called r, is identified by 4 points: $A(x_A,y_A)$, $B(x_B,y_B)$, $C(x_C,y_C)$ and $D(x_D,y_D)$, such as point D can be determined based on three other points as follows: $x_D=x_C+x_B-x_A$ and $y_D=y_C+y_B-y_A$. Each rectangle r is encapsulated in another, normal, called R as shown in figure 3. The rectangles r are grouped together in the set Rhl (formula 7), this set consists of two classes Rhl_a and Rhl_b which are defined as follows:

$$Rhl_a = \{r \in Rhl / (y_B \geq y_C \text{ and } x_A \geq x_D) \text{ OR } (y_B \leq y_C \text{ and } x_A \leq x_D)\ \} \quad (8)$$

$$Rhl_b = \{r \in Rhl / (y_B > y_C \text{ and } x_A < x_D) \text{ OR } (y_B < y_C \text{ and } x_A > x_D)\ \} \quad (9)$$

Each class has two subclass; the first one is grouping the rectangles oriented to the left named Rhl_{aL} and Rhl_{bL}(figure 6(a) and 6(c)) defined, respectively, by the formulas 10 and 12. The second includes those oriented to the right named Rhl_{aR} and Rhl_{bR} (figure 6(b) and 6(d)) expressed by 11 and 13.

Journal of Theoretical and Applied Information Technology
10th August 2015. Vol.78. No.1

ISSN: 1992-8645 www.jatit.org E-ISSN: 1817-3195

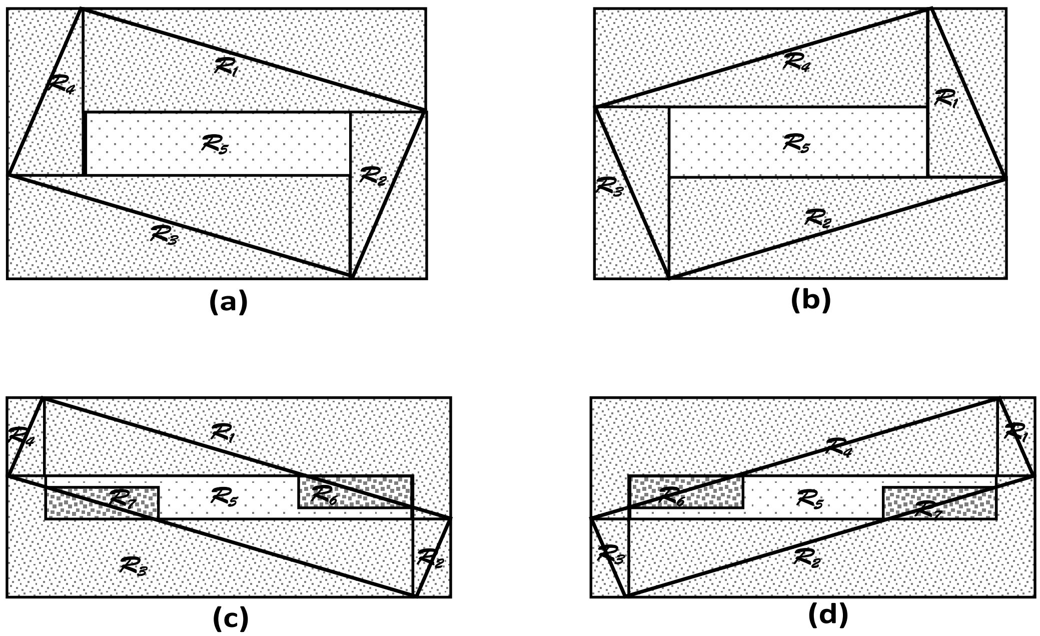

Figure 6: Representation of the rotated rectangle of (a) class RhlaL, (b) class RhlaR, (c) class RhlbL and (d) class RhlbR.

$$Rhl_{aL} = \{r \in Rhl_a / y_B \leq y_C \text{ and } x_A \leq x_D\} \quad (10)$$

$$Rhl_{aR} = \{r \in Rhl_a / y_B \geq y_C \text{ and } x_A \geq x_D\} \quad (11)$$

$$Rhl_{bL} = \{r \in Rhl_b / y_B > y_C \text{ and } x_A < x_D\} \quad (12)$$

$$Rhl_{bR} = \{r \in Rhl_b / y_B < y_C \text{ and } x_A > x_D\} \quad (13)$$

So we deduced that: $Rhl_a = Rhl_{aL} \cup Rhl_{aR}$ and $Rhl_b = Rhl_{bL} \cup Rhl_{bR}$.

4.2.2 Computing the Integral Image

As already mentioned, the rectangle R is split into several normal rectangles called R_i. As shown in figure 6, the Rhl_a category allows the division into five rectangles while Rhl_b category allows seven. Then theoretically the integral image value of the rectangle r, for both categories, is expressed by the following equations:

$$Rhl_a: \quad I_r = \sum_{i=1}^{4} I_{t_i} + I_{R_5} \quad (14)$$

$$Rhl_b: \quad I_r = \sum_{\substack{i=1 \\ i\neq 5}}^{7} I_{t_i} - I_{R_5} \quad (15)$$

Where: I_{t_i} are integral images of triangles t_i such as i=1, 2, 3, 4, 6 or 7. t_i is half of the rectangle R_i that intersects r (figure 7). I_{R5} is the one of the rectangle R_5. But, practically, the calculation of these integral images is very difficult if the angle α is different from 45° and will have a very important execution time which takes away, to the technique of the integral image, its simplicity and rapidity. For this reason we have calculated them with an approximate way as follows: $I_{t_i} = \frac{1}{2} I_{R_i} / i \in \{1,2,..,7\} - \{5\}$, Where: I_{R_i} is the integral image of rectangle R_i. So the two formulas (14) and (15) become:

$$Rhl_a: \quad I_r = \frac{1}{2}\sum_{i=1}^{4} I_{R_i} + I_{R_5} \quad (16)$$

$$Rhl_b: \quad I_r = \frac{1}{2}\sum_{\substack{i=1 \\ i\neq 5}}^{7} I_{R_i} - I_{R_5} \quad (17)$$

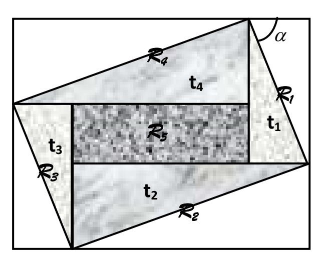

Figure 7: Representation of the rectangle r, rotated by an angle α. r is divided into four triangles and one rectangle in the middle for class Rhla and six triangles and one rectangle in the middle for class Rhlb.

Journal of Theoretical and Applied Information Technology
10th August 2015. Vol.78. No.1

ISSN: 1992-8645 www.jatit.org E-ISSN: 1817-3195

So in this way, we preserve the main advantage, for which the integral image is given for the first time by Viola and Jones, which consists of minimizing the memory access. The number of access is 12 for class Rhl_a, and 18 for class Rhl_b.

4.2.3 Discussion

In addition to the two above mentioned advantages, which are speed and simplicity, our technique allows involving the neighbouring pixels of the rectangle in computing of the integral image and this is very important because any component of the object to detect cannot be isolated from its environment. Take for example the detection of faces; a face consists of several determinant components such as the eyes, nose, mouth, etc. If we consider a rotated rectangle on an eye as shown in figure 8, the value of the integral image of this rectangle also helps to inform us about the eyebrows and eyelashes also. And this, of course as we believe, provides a wealth of information about a rectangle. And more if we consider the Rhl_b category, the calculation is performed by the intervention, on several occasions, of the pixels forming the rectangle, and this allows them to acquire a very important weight compared to neighbouring pixels.

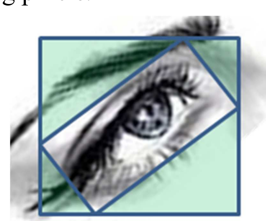

Figure 8 : Rectangle and its surroundings.

5. EXPERIMENTAL RESULTS

5.1 Test results and statistics

In this section we present some statistics on the results obtained by applying the method explained in section 3. The results are given relative to types of normal Haar-like features showed in figure1.

Table 1 shows a comparison with the method used by Lienhart et al. [8] and that proposed by Barczak et al. [9]. The results show that with our method, we can use a large number of features of different angles in the construction of detector, which can reach a difference of 47874 features with these methods, which increases its performance in detecting objects at different poses.

Table 1: Comparison with other methods

Types of features	Lienhart (45°)& Barczack (26,57°)	Our method			Differences
		45° & 26,57°	Other angles	Total	
A	18302	18302	13432	31734	**13432**
B	18302	18302	13432	31734	**13432**
C	10828	10828	5434	16262	**5434**
D	10828	10828	5434	16262	**5434**
E	8152	8152	4520	12672	**4520**
F	7150	7150	2388	9538	**2388**
G	7150	7150	2388	9538	**2388**
H	2826	2826	846	3672	**846**
Total	83538	83538	47874	131412	**47874**

Table 2 shows the number of rotated rectangles by a given angle for the type A. As we can see, the total number of angles obtained for the type A is 50, obviously it's a big number. Table 3 shows the number of angles used for each type.

Table 2: Angles used for type A (57)

*A	*N	A	N	A	N	A	N
45	10626	**12,53**	48	**59,04**	229	**41,19**	2
26,57	3838	**71,57**	1766	**51,34**	148	**82,87**	134
18,43	1766	**56,31**	1050	**39,81**	60	**69,44**	54
14,04	930	**36,87**	380	**35,54**	35	**57,99**	18
11,31	532	**30,96**	229	**32,01**	18	**48,81**	2
9,46	312	**23,2**	93	**29,05**	5	**83,66**	81
8,13	206	**20,56**	54	**80,54**	312	**77,47**	48
7,13	134	**16,7**	8	**50,19**	60	**66,04**	14
6,34	81	**75,96**	930	**40,6**	20	**60,95**	5
5,71	40	**53,13**	380	**81,87**	206	**84,29**	40
5,19	11	**38,66**	148	**74,05**	140	**73,3**	8
63,43	3838	**29,74**	58	**66,8**	93	**84,81**	11
33,69	1050	**23,96**	14	**60,26**	58		
21,8	342	**78,69**	532	**54,46**	35		
15,95	140	**68,2**	342	**49,4**	20		

**A: Rotation angle*
**N: Number of rectangles for the angle A*

Table 3: Number of angles used for each type of feature

Type of feature	Number of the angles
A	57
B	57
C	27
D	27
E	41
F	17
G	17
H	17

ISSN: 1992-8645 www.jatit.org E-ISSN: 1817-3195

These statistics show that our algorithm allows us to use a maximum number of different sized features and rotated by a variety of angles between 0° and 90°. These angles varies according to the resolution of the training window what has allows us to detect faces in different poses.

5.2 Practical examples

The algorithms proposed in this paper are designed to detect any type of object in an image. So to evaluate the robustness of these algorithms, we tested them for faces detection.

5.2.1 Training data

In our test, we have used two databases that are Umist [17] and CMU-PIE [16] which contains frontal and rotated faces. These faces are rotated by different angles and were subjected to changes in contrast, light etc. Also are scaled to a resolution of 24x24 pixels. The Umist database contains 6900 Images while CMU-PIE contains 9996.

The non-face examples used to train a classifier were extracted online from 3020 images of sizes varying from 320x240 to 512x512, in which there is no face. In our experiments, the training dataset and the testing dataset are completely separated and non-overlapped.

5.2.2 Results

In our experiments, two different cascades of face detectors are trained and evaluated. The first one that we called Umist-Detector, is trained by Umist set and is composed from 20 stages, the second is trained by the CMU-PIE set and is composed from 14 stages, we refer to this detector as PIE-Detector.

For the evaluation of the performance of our faces detector, we used, as most of other methods, MIT + CMU rotated test set [14] that we can easily find in [15]. This test set is one of the most commonly used datasets for assessing the performance of face-detection algorithms. This dataset is composed of 180 images containing about 500 faces of different sizes and poses. The large variations in image quality and in the scale of the faces greatly increase the difficulty of the face-detection task. Post-processing was the same as in [6]. The experiments were done on a 2.40GHz Intel Core i3 PC with 4 GB memory.

To compare our face detectors accuracy, we constructed the ROC curves shown in figure 9.

The majority of faces contained in the PIE database are Asian, for this reason PIE-Detector has difficulty to detect the faces of the MIT+CMU test set. Indeed it can be noted that the detection rate of UMIST-Detector is better than that of PIE-Detector. And also, according to the results presented in [4], [8] and [10], our detectors present detections rates better than those given by Viola, Lienhart and Barczack.

At the end of this paper you will find the figure 10 that illustrates some detection results using our Umist- detectors based on the MIT+CMU test sets.

6. CONCLUSION AND FUTURE WORK

In this paper, we have proposed a method to determine a large number of rotated Haar-like features by any angle. This number varies according to the size of the training window. We have also proposed a new method that calculates the approximate value of the rotated integral image; this has allowed us to keep the two major characteristics for which the integral image is proposed for the first time, which are: simplicity and speed.

To evaluate our algorithm we have tested it on two widely known databases; CMU-PIE set and Umist set, and as we have noted above, our algorithm presents detections rate better than that obtained by other methods such as those of Lienhart and Barczak.

Our perspectives are manifested by two challenges. The first is to improve the training time, for this reason we are working on optimizing the overall number of Haar-like features. The second one is to test our method on other disciplines such as Hand Tracking, detection of pedestrian, vehicle detection, etc.

REFRENCES:

[1] M. Oren, C. Papageorgiou, P. Sinha, E. Osuna, and T. Poggio. “Pedestrian detection using wavelet template”. In computer Vision and Pattern Recognition, pages 193-99, 1997.

[2] S.Mallat. “A theory for multiresolution signal decomposition: The wavelet representation”. IEEE Transactions on pattern Analysis and

ISSN: 1992-8645 www.jatit.org E-ISSN: 1817-3195

Machine Intelligence, 11(7):674-93, July 1989.

[3] S. L. Phung, A. Bouzerdoum, and D. Chai, “Skin segmentation using color pixel classification: Analysis and comparison”, PAMI, vol. 27, no. 1, pp. 148-154, 2005.

[4] P. Viola and M. Jones “Rapid Object Detection Using a Boosted Cascade of Simple Features”, IEEE Computer Society Conference on Computer Vision and Pattern Recognition, Vol. 1, pp. 511-518, 2001.

[5] M. J. Jones and P. Viola, “Robust real-time object detection” Tech. Rep. CRL-2001-1, Hewlett Packard Laboratories, Feb. 25 2001.

[6] P. Viola and M. J. Jones. Robust real-time face detection. Int. J. Comput. Vision, 57(2):137–154, 2004.

[7] M. J. Jones and P. Viola, “Fast multi-view face detection” Tech. Rep. TR2003-96, MERL, July 2003.

[8] R. Lienhart and J. Maydt, “An Extended Set of Haar-like Features for Rapid Object Detection”, IEEE ICIP 2002, Vol. 1, pp. 900-903, 2002.

[9] A. L. C. Barczak. “Toward an Efficient Implementation of a Rotation Invariant Detector using Haar-Like Features”, Proceedings of the IEEE/RSJ international conference on Intelligent robots and systems, Nouvelle-Zélande, Dunedin, 2005

[10] C. H. Messom, A. L. C. Barczak, “Stream processing for fast and efficient rotated Haar-like features using rotated integral images”. IJISTA 7(1): 40-57 (2009).

[11] C. H. Messom, A. L. C. Barczak, “Stream Processing of Integral Images for Real-Time Object Detection”. PDCAT 2008: 405-412.

[12] S. Du, N. Zheng, Q. You, Y. Wu, M. Yuan, and J. Wu, "Rotated Haar-Like Features for Face Detection with In-Plane Rotation", 12th International Conference, VSMM 2006, Xi’an, China, October 18-20, 2006. Proceedings, pp 128-137.

[13] G. A. Ramirez, O. Fuentes, “Multi-Pose Face Detection With Asymmetric Haar Features”, Applications of Computer Vision, WACV, 2008, IEEE Workshop in Copper Mountain,CO.

[14] Rowley, H., Baluja, S., Kanade, T.: “Neural network-based face detection”, In IEEE Trans. Pattern Analysis and Machine Intelligence, 20 (1998) 23–38.

[15] CMU/VASC Image Database: “http://vasc.ri.cmu.edu/idb/html/face/frontal_images/”.

[16] PIE DataBase : “http://www.ri.cmu.edu/research_project_detail.html?project_id=418&menu_id=261”.

[17] Umist Database: “http://www.sheffield.ac.uk/eee/research/iel/research/face”

ISSN: 1992-8645 www.jatit.org E-ISSN: 1817-3195

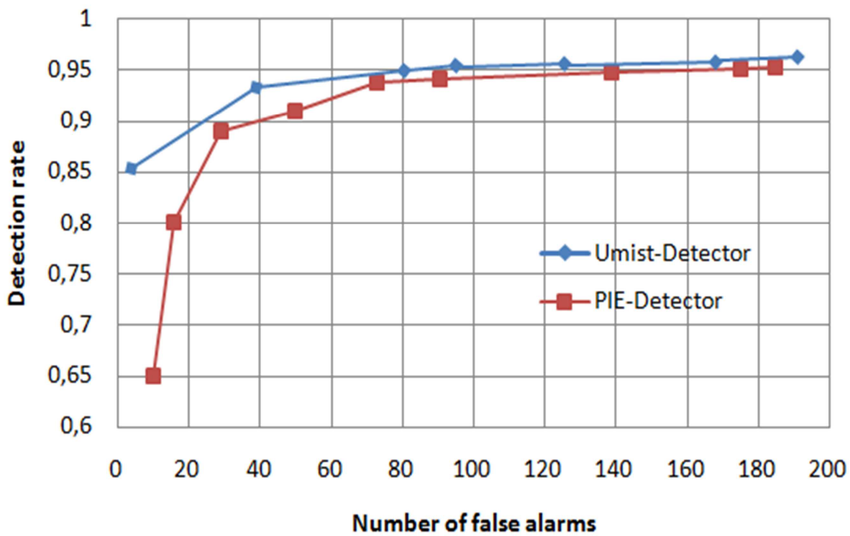

Figure 9: The ROC curves of the Umist-Detector and the PIE-Detector using the MIT + CMU test set.

Figure 10: Some detection results using our Umist-Detector on the MIT + CMU test set.